Granular Matter (2013) 15:827–840
DOI 10.1007/s10035-013-0445-5

ORIGINAL PAPER

Characterization of fluctuations in granular hopper flow

Guilhem Mollon · Jidong Zhao

Received: 7 May 2013 / Published online: 20 September 2013

Abstract We present a 2D discrete modelling of sand flow through a hopper using realistic grain shapes. A post-processing method is used to assess the local fluctuations in terms of void ratio, coordination number, velocity magnitude, and mean stress. The characteristics of fluctuations associated with the four considered quantities along the vertical axis of the hopper and across the entire hopper are carefully examined. The flow fluctuations for coordination number, velocity magnitude and mean stress are all found to take the form of radial waves originating from the lower centre of the hopper and propagating in the opposite direction of the granular flow. Quantitative characteristics of these waves (shape, amplitude, frequency, velocity, etc.) are identified. The fluctuations in void ratio however are not supportive of the observation of density waves in the granular flow as mentioned in some experiments. The possible reasons for this apparent contradiction are discussed, as well as possible extensions of this work.

Keywords Granular flow · Fluctuations · Hopper flow · Complex particle shapes

1 Introduction

The flow of granular media is of great interest for a wide range of engineering and industrial branches, such as civil, mining and chemical engineering, pharmaceutical and powder industries. Effective characterization of a dense equilibrium granular flow is also a challenging scientific problem in condensed matter physics and geophysics. Continuous efforts have been made towards defining the constitutive equations to describe the flow of such materials (see for example [1] for a complete review). In addition to classical approaches which are chiefly based on experimental tests, particle-based discrete modeling of medium-to-large-scale granular systems using Discrete Element Method (DEM) or Molecular Dynamics (MD) approach has been the current trend of research in this field [2]. DEM has indeed been extensively applied to the investigation of a variety of flow-related problems such as chute flows [3], pipe flows [4], flows on inclined planes [5,6], rock avalanches [7,8], and flat-bottom hopper flows [9].

A particularly interesting case of granular flow is the one occurring through a wedge-shaped or conical hopper. The classical hourglass problem is a good example of this kind. Despite its simplicity in geometry, the hopper granular flow under gravity may present rather complicated behavior which draws great attention from the community of physics and engineering sciences. Hopper flow has been repeatedly treated both theoretically (see, e.g., [10–13]) and experimentally (see [14–20]), as well as numerically by DEM [21–23]. One peculiar aspect of a hopper flow frequently reported is the observation of strong fluctuations in the velocity field. This phenomenon was first observed experimentally by Baxter et al. [15] who proposed the theory of decompression waves propagating upwards at a much higher speed than the flow itself to describe the phenomenon. It was also observed that the wave velocity tends to increase if the opening angle of the hopper is reduced, and that the waves do not occur at all if the sand particles are very rounded. Such waves were also observed by Gardel and et al. [17,18] based on experiments on glass and steel beads. They reported that the velocity

G. Mollon (✉)
3SRLab, CNRS UMR5521, UJF Grenoble 1, Grenoble INP,
Domaine Universitaire, 38041 Grenoble, France
e-mail: guilhem.mollon@gmail.com

J. Zhao
Department of Civil and Environmental Engineering,
Hong Kong University of Science and Technology,
Clearwater Bay, Kowloon, Hong Kong

fluctuations are spatially correlated and this correlation is anisotropic (more correlation in the direction transversal to the flow than in the direction of the flow). They also measured a negative correlation between the velocities and the stresses at a given point, and attributed the fluctuations to collisional chains between the grains. More recently, Vivanco et al. [20] conducted 2D photoelastic experiments and showed that the velocity fluctuations could be attributed to an intermittent network of arches and force chains. They also showed that the fluctuations tend to disappear if the opening width of the hopper is large enough, most probably because it reduces the ability of the material to develop these arches. Based on their observations, they proposed the following heuristic theory to explain these fluctuations: during the flow, the force chains may develop from the lateral walls, and these chains may join to form arches across the hopper; these arches may then reduce the velocity of the flow, until they break because of the load and momentum of the particles above, which would trigger an acceleration of the flow and ease the formation of new force chains. This heuristic theory is indeed similar to the one proposed earlier by Baxter et al. [15]. The experimental observations were further reproduced by Ristow and Herrmann [21] based on DEM simulations where they showed that such fluctuations do not occur in frictionless material, probably because no strong force chains can be established in the flow. Cleary and Sawley [23] reported similar fluctuations in their DEM simulations using non-circular particles, and their primary interest was focused on the influence of fluctuations on the forces acting on the lateral walls. These forces are most important to chemical and mining industries using hoppers and silos where the relevant structures are known to be fragile when subjected to vibrations induced by the fluctuations of the flow. In addition, vortex-like displacement fluctuations were reported in quasi-static shearing of granular materials [24–26], but no direct evidence has shown that such fluctuations are related to the "waves" observed in hopper flows.

In this paper, we present a two-dimensional DEM study of sand flow through a wedge-shaped hopper, based on realistic reproduction of the shape of sand particles using a Fourier-Voronoi approach (Mollon and Zhao [27]). The use of realistic particle shape in the simulation may help to reproduce the real hopper flow behavior better than many studies that use circular or simple non-circular (e.g., elliptical) particles. The primary focus of the study is placed on detailed observations and characterization of the fluctuations of the simulated hopper flow in an attempt to identify interesting features and correlations of different local quantities that may help understanding the hidden physical mechanisms. Towards post-processing and interpreting the DEM simulation results on granular flow, a commonly followed approach is to employ some representative elementary volumes (REVs) to compute the averaged quantities of interest. Depending on the size of the RVE, these obtained quantities can be treated as either local or global variables (e.g. stress, strain, local/global void ratio, etc.). Frequently these quantities are computed at a given moment in time, and in some cases they are averaged over a given time interval. However, it is known that a granular hopper flow is multi-scale in nature in both space and time. It proves to be difficult and challenging in many cases to ascertain the suitable resolutions in time and/or the size of RVE for accurate descriptions of the behavior of granular hopper flow. Aiming to address this outstanding issue, we propose in this study a robust and novel post-processing methodology using statistical tools in an attempt to better characterize the spatial and temporal fluctuations in granular flow. Based on this method and chosen statistical quantities, it is hoped that some unique and coherent characteristics associated with granular hopper flow can be identified to help us gain insights into the complex phenomena observed in the flow process. It is noted that our study is confined to two-dimensional which may appear to be overly simplified compared to real engineering applications. A more realistic modeling of a real hopper flow (such as the ones encountered in the mining industry, for example) may require a full 3D simulation involving realistic grain shapes. The present study is targeted to account for the complexity of particle shape as a very first step, and to further consider the three-dimensional simulation in a future work. The methodology described in this paper can be conveniently translated into formulations which are applicable to 3D simulations.

2 Simulation

As mentioned before, to capture the behaviour of real engineering particles such as sand flowing through a hopper, the first important step is to reproduce the particle shape in a robust manner. We employ here the Fourier-Voronoi approach recently proposed by Mollon and Zhao [27] to prepare the sand particles for the subsequent hopper flow simulation. The novelty of this Fourier-Voronoi method lies in its rigorous consideration of key statistical characteristics, relevant to particle shapes and grain size distribution identified from experimental data on granular particles such as sand, in generating granular packing for discrete modeling. Specifically, particles with different shapes are randomly generated based on Fourier spectrums obtained experimentally (e.g., for sand, Das [28]), and are then packed in a container of arbitrary geometry using a cell-filling approach based on constrained Voronoi tessellation to ensure a realistic size distribution of the particles. A final step to furnish the method is to fill each particle so generated with multiple discs of varied diameters based on the ODEC framework (Ferellec and McDowell [29]), which facilitate them to be directly introduced in a

DEM code. The source code of the program is available for download at http://guilhem.mollon.free.fr.

This method is employed in the present paper to generate an assembly of Toyoura sand in a hopper container. Toyoura sand is chosen for its common use in the field of geomechanics. Relevant Fourier spectrums of Toyoura sand are based on those reported by Das [28] (see also Mollon and Zhao [31]). The generated sample consists of roughly 6,000 particles of average diameter $D = 0.25$ mm (the "diameter" of a particle with complex shape is determined by the distance from its centre to its average edge all around its contour, as detailed in [27]). The generation Matlab software is tuned to match the actual size distribution (via the coefficient of uniformity $C_u = 1.24$), the material density (2.65) and the Fourier spectrums of Toyoura sand. The considered hopper has a constant opening angle equal to 60°, and an opening width equal to $15D = 3.75$ mm. The contact law implemented in the DEM code is a classical viscous-frictional law, with an interparticle and wall-particle coefficient of friction equal to 0.4 and an equivalent coefficient of restitution equal to 0.3. The contact stiffness is set to 10^5 for every contact in the simulation. The generated sample first settles down under gravity, and the flow is then triggered by removing the lower cover of the hopper outlet. A snapshot of the granular system during the flow is presented in Fig. 1. In a recent conference paper [30], we made a comparison between the flows of circular and complex particles, without discussing the flow fluctuations in detail. Using non-circular particles for the simulation of granular flow appears to lead to reduced flow-rate, considerable changes of the velocity field towards the funnel, localized particles rotations, increased coordination number and complicated behaviors in shear stresses and fabric anisotropy. These observations are consistent with the observed characteristics in real hopper flows. For this reason, realistic shapes are chosen in the present simulation instead of simple circular ones. As each simulation with the complex particle shape is rather time-consuming, only one simulation has been performed to save computational and post-processing cost. While the current study is focused on quantifying the flow properties and fluctuations by a robust post-processing methodology, if statistical consistency of the hopper flow characteristics is of major concern, it is desirable to carry out several realizations of the simulation to gain high confidence. This goal will be pursued in the future.

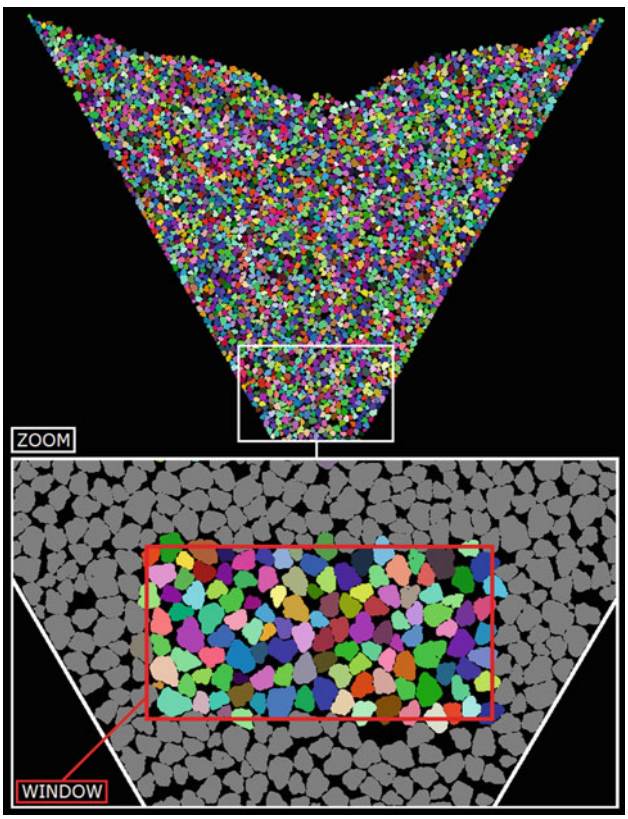

Fig. 1 Overview and zoom on the proposed 2D discrete simulation of sand flow through a hopper

3 Observation of fluctuations on a vertical profile

Velocity fluctuations in a hopper flow have been described in the scientific literature as waves propagating upward from the hopper outlet to the free surface of the granular material. To accurately quantify the fluctuations in seeking for deeper insights of their behavior, a specific post-processing method is chosen in this study. In particular, observation "windows" are used to quantify the local flow properties. Such a window, as shown in Fig. 1, is a rectangle with a width of $15D$ and a height of $8D$. Only those particles with a mass centre located inside the window are considered to be within. In our simulations, the typical number of particles inside such a window is close to 100. Four quantities are then tracked: the void ratio, the coordination number, the average magnitude of velocity and the mean stress. The dimensions of this observation window have been chosen to contain a large enough number of particles. It was also chosen to have a smaller height than width, since it was demonstrated by Gardel et al. [18] that the flow fluctuations are much more correlated in the horizontal direction than in the vertical. However, it does not ensure that the flow properties are uniform inside this kind of window. To improve the relevance of our results, we have further run a number of tests to evaluate the variability of the velocity magnitude within such a window for all positions considered in the paper. It appears that the average coefficient of variation (COV, equal to the standard deviation divided by the mean value) of the velocity magnitude of the particles within a given window is close to 11 %. In the lower part of the flow it is closer to 16 % (because the velocity vertical gradient is larger in this area), while in the central part of the hopper the COV is closer to 7 %. Based on these results, we believe that

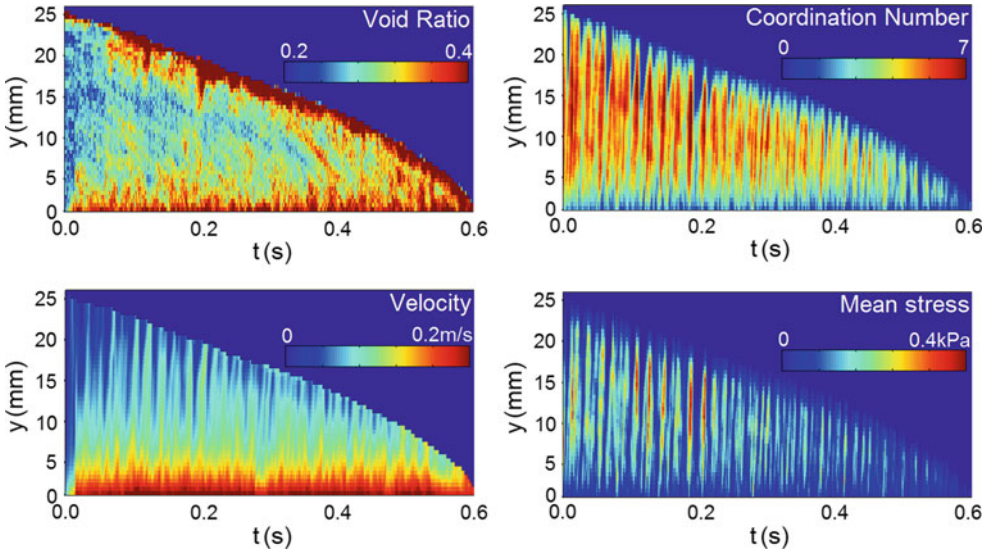

Fig. 2 Space–time diagrams of the void ratio, the coordination number, the velocity magnitude, and the mean stress, on the *vertical axis* of the hopper during the whole flow

these observation windows provide consistent estimators of the local flow properties.

Based on the method described in [8], the void ratio e is computed by enveloping the particles inside a close non-convex 2D contour and then measuring the area S_t of the non-convex surface and the area S_p of the sand particles:

$$e = \frac{S_t - S_p}{S_p} \tag{1}$$

The coordination number is taken as the average number of contacts per particle inside the window, and thus accounts for the multi-contacts that often occur between a single pair of non-convex particles. The average stress tensor inside the window is obtained using the following formula:

$$\sigma_{ij} = \frac{1}{8D \cdot 15D} \sum_k F_i^k \otimes r_j^k \tag{2}$$

In this expression, F_i^k and r_j^k are the contact force and the branch vector joining the centres of the two particles in contact at a specific contact k. The sum is performed over all contacts located inside the window. The mean stress is then given by the first invariant of σ_{ij}:

$$\sigma_m = \frac{\sigma_{11} + \sigma_{22}}{2} \tag{3}$$

Finally, the average velocity magnitude is given by the following expression:

$$V_m = \frac{1}{n} \sum_{i=1}^{n} V_i \tag{4}$$

where n is the number of particles inside the window and V_i is the velocity magnitude of the ith particle.

The observation window is shifted along the vertical axis of the hopper to examine the instantaneous local values of these quantities in space. The vertical position of the window is defined by the vertical distance y from its centre at the hopper outlet. The operation is performed every 10^{-3} s from the beginning of the flow to the total discharge, and the results are recapitulated in the space–time diagrams plotted in Fig. 2. In each of these charts one can easily assess the position of the free surface, which corresponds to the upper limit of each graph in the y-axis at certain instant. Systematic fluctuations in the coordination number, the velocity magnitude and the mean stress are indeed apparent in this figure. At the chosen time-scale of observation, these three quantities vary in a systematical and coordinated manner along the vertical axis. The periodicity of the three quantities appears to be rather consistent. While the void ratio evolves in space in a similar trend as the other three, its fluctuations do not appear to be either spatially coordinated or to exhibit any clear periodicity. The fluctuation in void ratio is more erratic than the other three cases. To improve the accuracy of the analysis, a narrower time interval has been adopted in the study. Instead of using a sampling time step of 10^{-3}, in what follows we consider the time-interval $[t_1; t_1 + 0.1\,\text{s}]$ with a sampling time-step of 10^{-4}. In the following analysis, we take t_1 as the instant corresponding to 0.05 s after beginning of the flow, and this instant will be treated as the origin of the time axis. Based on the observation from Fig. 2, this time interval is believed to be short enough to identify rather consistent characteristics of the flow and meanwhile long enough to observe adequate number of cycles on the fluctuations.

A direct observation of the fluctuations is provided in Figs. 3 and 4. Figure 3 shows the time-averaged distributions and standard deviations for the found quantities. An

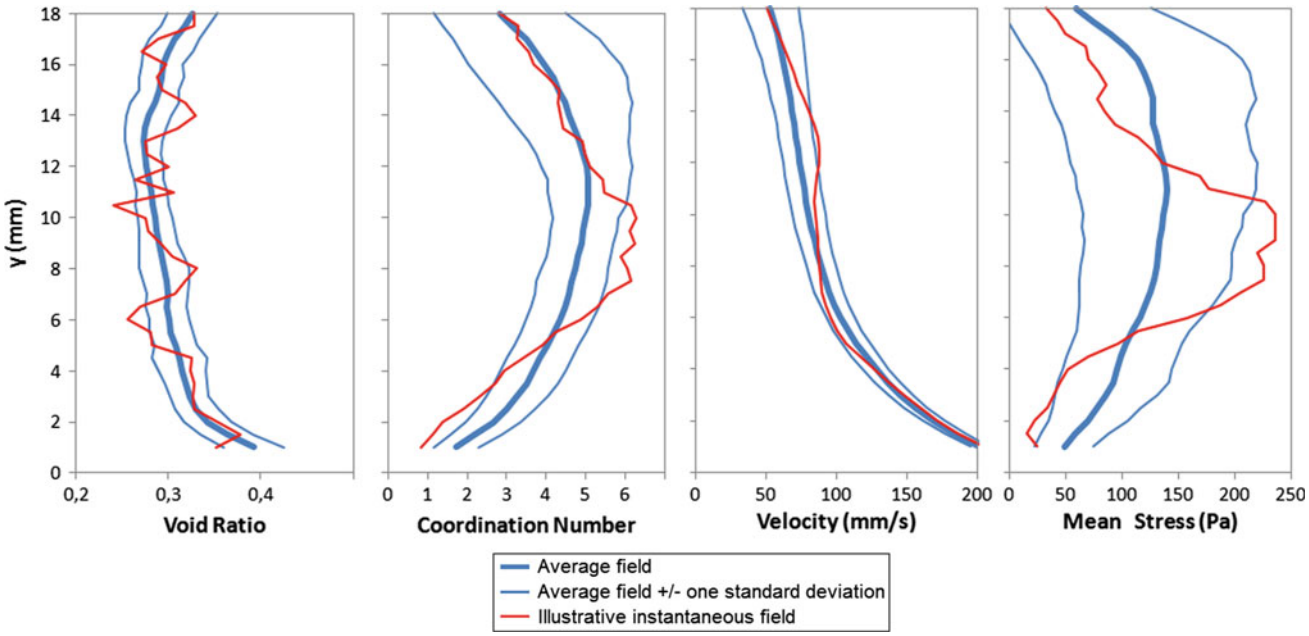

Fig. 3 Average fields and their standard deviations of the void ratio, the coordination number, the velocity magnitude, and the mean stress, on the *vertical axis* of the hopper; in *red*: instantaneous field at $t = t_1 + 32$ ms (color figure online)

illustrative instantaneous field (corresponding to the time $t = t_1 + 32$ ms) is also provided in each case. As is shown, the average void ratio is close to 0.3 and is rather constant across the vertical profile. It becomes slightly larger at the outlet and at the surface, due respectively to the decompression of the material before it is released from the exit and less overburden close to the free surface. The distributions of average coordination number and mean stress have a similar trend, exhibiting a peak at 2/3 of the profile and decreasing in value to both the surface and the bottom directions. The trend is indeed opposite to that of the void ratio. Meanwhile, both the mean stress and the coordination number show relative larger deviations at the top portion of the profile than at the bottom and the instantaneous distributions for them depict greater variations along the y axis than that of the void ratio. Compared to the above three, the average velocity profile presents a much smoother and steady increasing curve from the top to the outlet. The velocity close to the outlet increases apparently more dramatically than at higher location. The dispersion of velocity is also relatively smaller than the other three quantities.

Figure 4 presents the variations of the four quantities during the considered time interval, for an observation window located at y = 11 mm. The average value and the dispersion are also presented for each signal. The fluctuation pattern of the void ratio is evidently different from the other three quantities, which confirms the observations in Fig. 2. During the time interval, the evolution of void ratio shows rather confined fluctuations (varying between 0.25 and 0.32) without apparent periodicity. The fluctuation patterns of the three other quantities are more easily identifiable and the fluctuation ranges are also significantly larger (e.g., the coordination number varies between 3 and 7, the velocity magnitude varies between 50 and 100 mm/s, and the mean stress varies between 20 and 380 Pa). Interestingly, the variations of coordination number and mean stress with time appear to be well correlated in both periodicity and peak/valley pattern, which is consistent with the observation in Fig. 3.

4 Normalized fluctuations

It is observed from Fig. 3 that the mean value and the dispersion of relevant quantities of the granular flow vary considerably with location in the hopper. To describe the fluctuations more rationally, we employ a normalization approach on these quantities. Specifically, we normalize the difference between the current value of a concerned quantity and its time-averaged value by its standard deviation. According to this approach, for example, the following normalized void ratio $\tilde{e}$ is obtained:

$$\tilde{e} = \frac{e - \mu_e}{\sigma_e} \tag{5}$$

where μ_e and σ_e are the local mean value and standard deviation of the void ratio. The other three quantities are normalized in a similar way. In addition, by expressing the quantity of distance in terms of the average particle diameter D, the following classical representative quantities for time, velocity, stress, and force are introduced for further scaling:

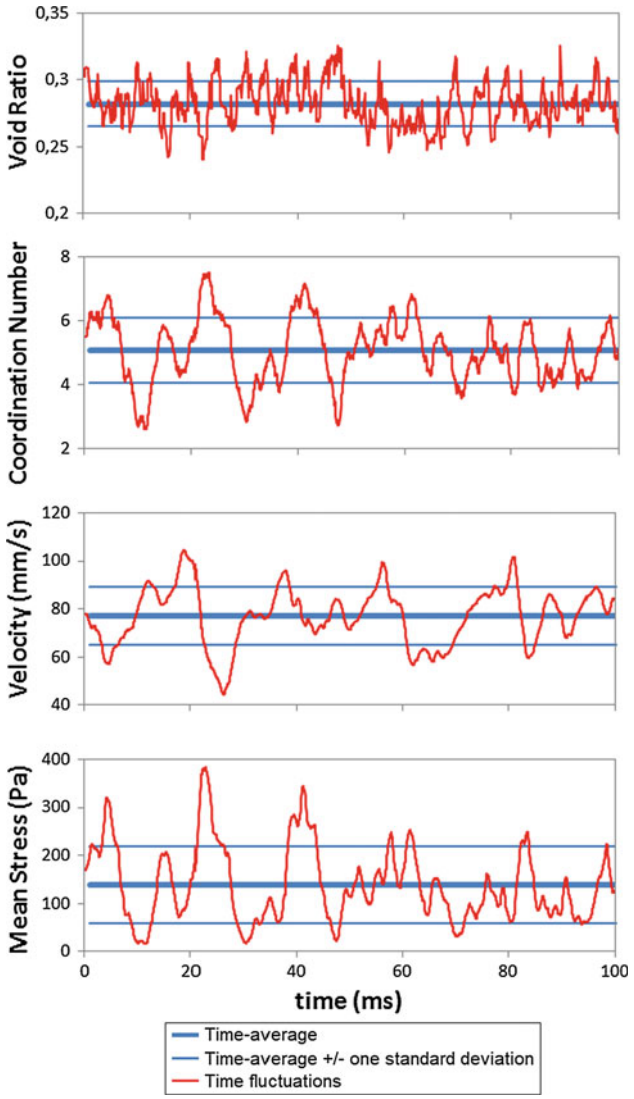

Fig. 4 Fluctuations in time of the void ratio, the coordination number, the velocity magnitude, and the mean stress, for an observation window located at y = 11 mm

$$t^* = \sqrt{D/g} \tag{6}$$

$$V^* = \sqrt{gD} \tag{7}$$

$$\sigma^* = \pi \rho g D/4 \tag{8}$$

$$F^* = \pi \rho g D^2/4 \tag{9}$$

Based on these definitions, the four quantities are normalized and re-plotted in Fig. 5 wherein the normalization operation apparently renders more information identifiable from observation of the fluctuations of these quantities. The coordination number, the velocity magnitude and the mean stress depict clearer "fluctuation waves" in this figure. With rather constant normalized (peak-to-peak) amplitude of around 4–6 standard deviations, these waves propagate upward at an apparently constant velocity. The normalized fluctuations of the void ratio do not exhibit such a wave pattern. The only structured fluctuation observable for void ratio is a downward propagation at a rather small velocity. This may be attributable to persistent granular structures of high or low density traveling down with the granular flow, which have been further observed from the videos of density field during the flow (not shown here).

The variations of these normalized quantities over time for a window located at a height y = $50D$ are further subjected to a discrete Fourier transform, and the obtained spectrums are plotted in Fig. 6. While the spectrum for the void ratio does not show any specific structure, those of the three other quantities demonstrate an interestingly similar mode of fluctuation, with an almost identical frequency at around $0.25/t^*$. We further repeat the operation by changing the location of the observation window, which leads to the plot in Fig. 7 with a third dimension of the location. It is evident that the evolution of the void ratio Fourier spectrum does not exhibit any particular distinguishable pattern along the vertical axis of the hopper. Though there are some peaks in the spectrum, they appear to be rather random in space and may be attributed to some fortuitous fluctuations in the void ratio. On the other hand, the spectrums of the coordination number, the velocity magnitude and the mean stress depict similar interesting patterns along the vertical axis, and the magnitude of the frequency peak for all three cases increases steadily with y (the vertical distance from the hopper outlet). This signifies a progressive structuration of waves traveling upwards during the granular flow, which start from relatively complex fluctuations at the hopper bottom (between 0 and 20D) to an almost harmonic pattern after a given traveling distance in the granular material (above 60D). The period is identified to be close to $4t^*$.

5 Correlations on a vertical profile

We further investigate the correlations between the normalized fluctuations of these four variables at a given point. We examine two types of correlations, one being instantaneous (i.e. the correlation between the time series of two variables for a given location of the observation window) and the other being sequential (i.e., the correlation for a given normalized variable between one time instant and the subsequent time instant after specific time delay/gap). The most relevant results obtained by this approach are presented in Fig. 8. The upper-left figure in Fig. 8 presents the correlation between the normalized fluctuations of the mean stress and those of the coordination number as a function of the delay of the latter, for an observation window located at $y = 60D$. The graph clearly indicates a good correlation between the normalized

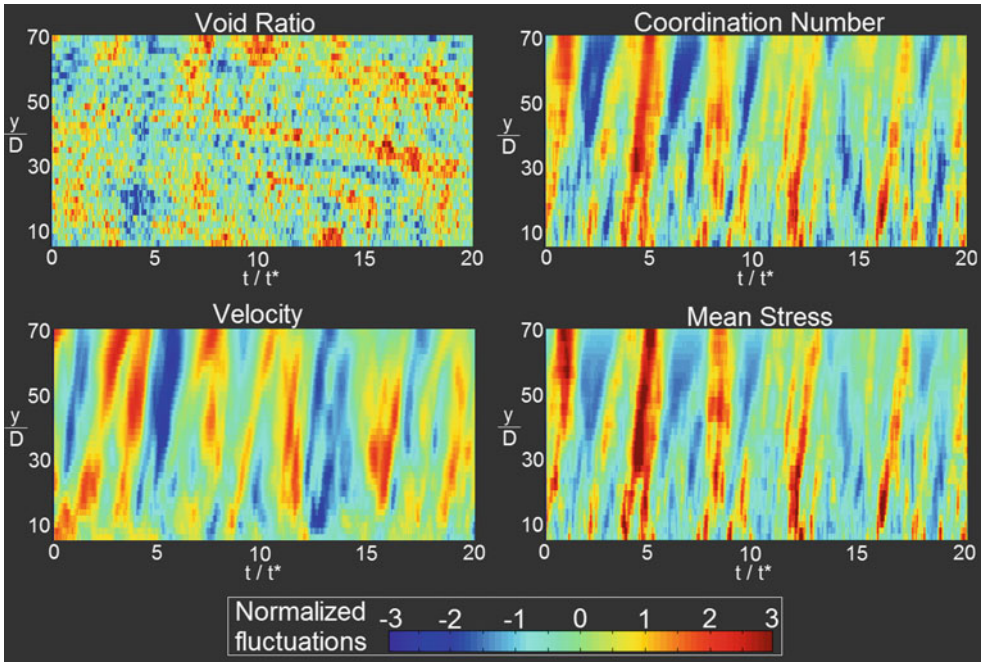

Fig. 5 Space–time diagrams of the void ratio, the coordination number, the velocity magnitude, and the mean stress, after normalization, during the restrained observation interval

fluctuations of the mean stress and those of the coordination number, and the two variables have perfectly synchronized period from this figure. The bottom-left figure of Fig. 8 shows the same data across the vertical axis, which indicates that this correlation and the feature of synchronicity are indeed valid everywhere along this axis. The two figures on the right of Fig. 8 show the same kind of curves for the correlations between the velocity magnitude and the mean stress. It is evident that the fluctuations of these two quantities are also coordinated but not completely synchronized, since the maximal correlation between the two signals is slightly delayed. For an observation window located at $y = 60D$, the fluctuations of velocity are strongly positively correlated (0.72) with those of the mean stress that occur roughly t^* later, and are strongly negatively correlated (-0.69) with the mean stress fluctuations that occur roughly $0.7t^*$ earlier. At a given time instant without delay (delay $= 0$), the correlation between the velocity magnitude and the mean stress is negative (-0.32).

The above observations provide supporting evidence to the heuristic theory proposed by [20], about the flow fluctuations being related to dynamic networks of force chains, as explained in the introduction of the present paper. Indeed, the correlations show that the occurrence of maximum velocity magnitude at a given instant t_0 is typically preceded by a minimum of the mean stress (and of the coordination number) at about $t_0 - 0.7t^*$, and is then followed by a maximum of mean stress at about $t_0 + t^*$. Similarly, a minimum of the velocity magnitude occurring at a given instant t_0 is typically bracketed by a maximum (at about $t_0 - 0.7t^*$) and a minimum (at about $t_0 + t^*$) of both the mean stress and the coordination number. In conjunction with the $4t^*$ periodicity found in the last section, this suggests that the formation of force chains (corresponding to an increase of coordination number and/or the mean stress) may cause significant reduction of the particle velocity (with a delay of roughly $0.7t^*$ to t^*) until these chains break down under the load and momentum of the particles above. The collapse of force chains leads to an increase of the velocity which in turn would induce the formation of new force chains that break down again later. Such periodic circles feature the process of granular flow in the hopper. The bottom-right figure of Fig. 8 also indicates that this phenomenon becomes more intense at the upper part of the hopper than at the bottom, since the amplitude of the correlation increases with height (from the bottom). These results suggest that the fluctuations commonly observed in a hopper flow involve close correlations between coordination number, velocity magnitude and mean stress with interesting underlying physical mechanisms. However the role of void ratio in these fluctuations remains unclear.

The study of correlations also offers a good way to evaluate the characteristics of wave propagation during a hopper granular flow. Figure 9 shows the delayed correlation between the normalized fluctuations of the velocity magnitude at several heights (each curve corresponding to a given height of the observation window indicated in the figure in terms of average diameter D) and the velocity fluctuations at $y = 20D$. This reference height is chosen due mainly to the observation from Figs. 7 and 8 that it is the smallest height for which the fluctuations are structured. The height $y = 20D$ may hence be considered as the "emission point" (or source)

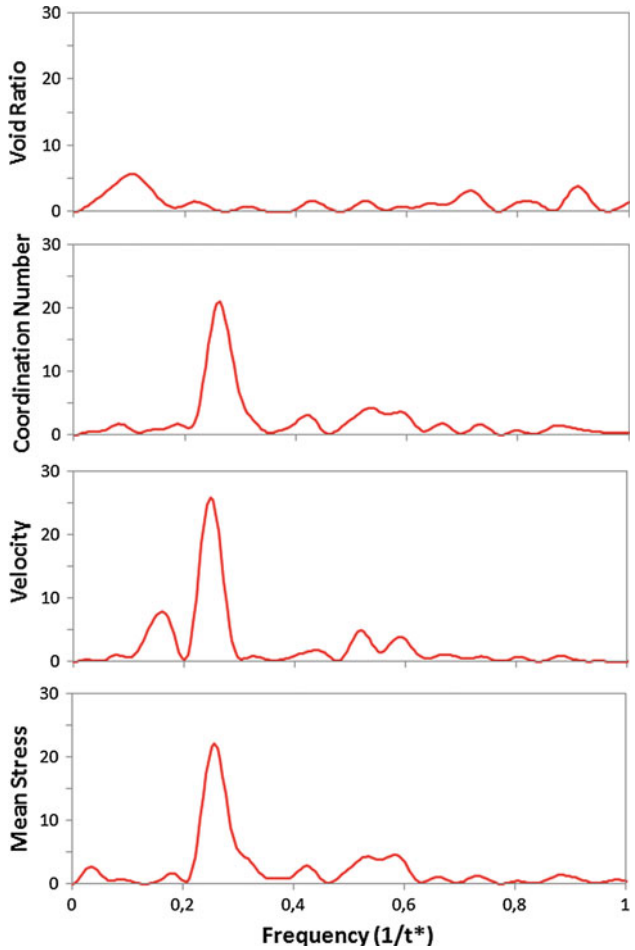

Fig. 6 Fourier spectrums of the time-signals of the void ratio, the coordination number, the velocity magnitude, and the mean stress, for an observation window located at y = 11 mm

of these waves. As shown in Fig. 9, for a given height of the observation window, the maximum correlation of the local normalized fluctuations of the velocity magnitude with the one at $y = 20D$ is delayed in time. This delay is related to the average time of travel of the wave from $y = 20D$ to the considered height. In the inset of Fig. 9, the time-space positions of these maximums of correlation are plotted which show that the average distance of wave traveling is linear in time, indicating a constant wave propagating rate. A linear regression provides an average traveling rate equal to $54.1V^*$, which is much larger than the velocity magnitude of the grains (between $0.2V^*$ and $4V^*$ depending on the location in the hopper, see Fig. 11 for more details).

6 Spatial structure of the fluctuations

The discussion in previous sections focuses on the flow fluctuations along the vertical axis of the hopper. It is meanwhile interesting to explore the behavior of granular flow in the transversal direction. To this end, a fixed polar mesh is defined in Fig. 10. The mesh consists of 621 homogeneous cells, each cell containing 5–10 particles at a given time. The same post-processing methods as described in Sect. 3 are used, except that the previously defined "observation window" in Fig. 1 is now replaced by a new window formed by any one of these "cells" together with its closest neighboring cells (eight neighboring cells in the center part, five at the hopper walls, and three at the corners). This method ensures that each observation window contains 50–80 particles and that the measured quantities (void ratio, etc.) are locally representative. The time-averaging interval and the sampling rate are the same as in previous sections. This time-interval is kept because the mesh is constantly filled with matter (i.e. the free surface never crosses the mesh).

Figure 11 provides the mean and the coefficient of variation (COV, equal to the standard deviation normalized by the mean value) of the void ratio, the coordination number, the velocity magnitude and the mean stress, in all the cells of the polar mesh. The distributions of the mean value and COV of the void ratio appear to be rather random in the hopper, with a rather low dispersion (COV close to 20 %), which confirms the observations from Fig. 3. The average velocity field shows a strong variation along the vertical axis (as is also seen in Fig. 3) and the transversal axis as well. While the central velocity can be large, the velocity in the neighborhood of the lateral walls of the hopper is vanishingly small. This narrow velocity field may be attributed to the strongly non-circular shapes of the particles used in the study which are known to easily induce this kind of "funnel flow". Interestingly, the fluctuations of the velocity field appear to be more intense in the areas where the velocity magnitude is low (i.e. in the upper and lateral zones of the hopper). The COV of the velocity magnitude may reach 60 % is these areas, while it is much smaller around the funnel and even close to zero when approaching the hopper outlet. As in previous sections, the coordination number and the mean stress appear to exhibit similar behaviors. Their average fields are very low in both the upper and lower parts of the hopper (because of the smaller burden in the upper part and the decompression close to the outlet), and are maximum close to the lateral walls. The COVs of these two quantities are rather uniform in the central part of the hopper (about 20 % for the coordination number and 60 % for the mean stress), but are more heterogeneous in the lower and upper part of the flow. These observations indicate a change of the flow regime in these areas, in which the force chains are much less persistent such that the sand may be considered as a "granular gas" with collisional interactions between particles dominating.

Figure 12 provides the spatial cross-correlations of the fluctuations of the four normalized fields. These normalized fields are obtained for each pixel (cell) in the same way as in Sect. 4. Six reference pixels at several locations along the vertical axis of the hopper (termed as A to F) are considered.

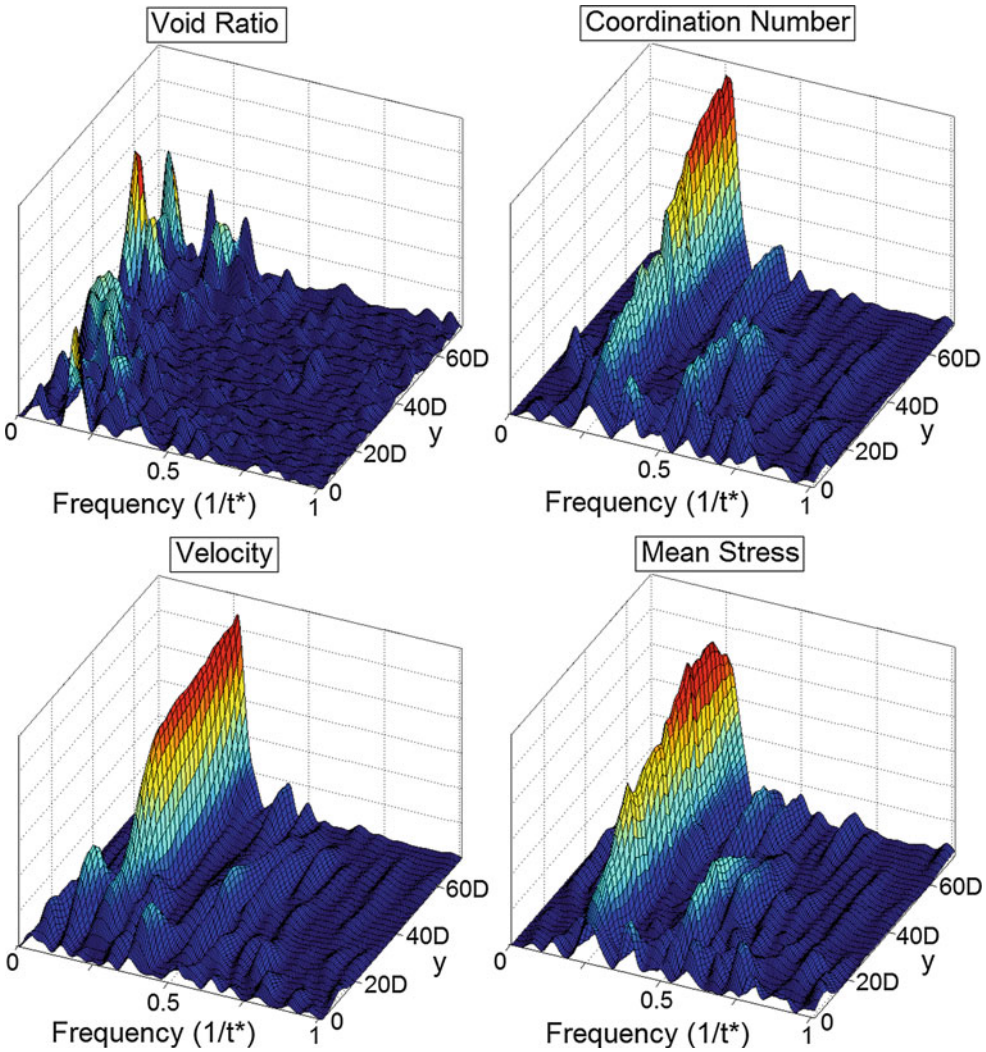

Fig. 7 Fourier spectrums of the time-signals of the void ratio, the coordination number, the velocity magnitude, and the mean stress, as a function of the height y of the observation window

The instantaneous correlations with the normalized fluctuations at these pixels are computed for all the other pixels of the mesh. The resulting cross-correlation fields are plotted for each of the six pixels and for each of the four quantities, leading to the 24 graphs of Fig. 12. The first line of this figure clearly shows that the void ratio fluctuations are not structured in space, since the cross-correlation coefficient of this field is close to zero everywhere in the hopper. The other three quantities show a very different behavior, with interesting cross-correlation patterns. The correlation distance is limited at lower parts of the hopper (e.g., Pixel A), but becomes significantly large when higher pixels are considered. In addition, a strong anisotropy is depicted in the correlation distances and is more intense in the transversal direction than in the vertical. This anisotropy increases with height, suggesting a progressive synchronization of the waves over the entire width of the flow when traveling upwards. The structure of the fluctuations appears to be radially orthotropic, especially for the mean stress and coordination number, which means that the propagation rate of the wave may be constant in any radial direction. In the upper part of the hopper (right-hand column of Fig. 12), the cross-correlation of the fluctuations is almost equal to 1 across the whole width of the hopper, indicating an almost perfect synchronicity between the normalized fluctuations at a given distance from the hopper outlet.

The evolution of contact forces network during a typical hopper flow is illustrated in Fig. 13. Fifteen snapshots of this network are provided at regular instants of the flow, running from $t/t^* = 1$ to $t/t^* = 3.8$ (in accordance with the time-scale proposed in Fig. 5). At $t/t^* = 1$, an arching pattern may be observed in the upper two-thirds of the hopper, while the lower one-third portion shows no clear arching (there are some contacts, represented by blue segments, but they do

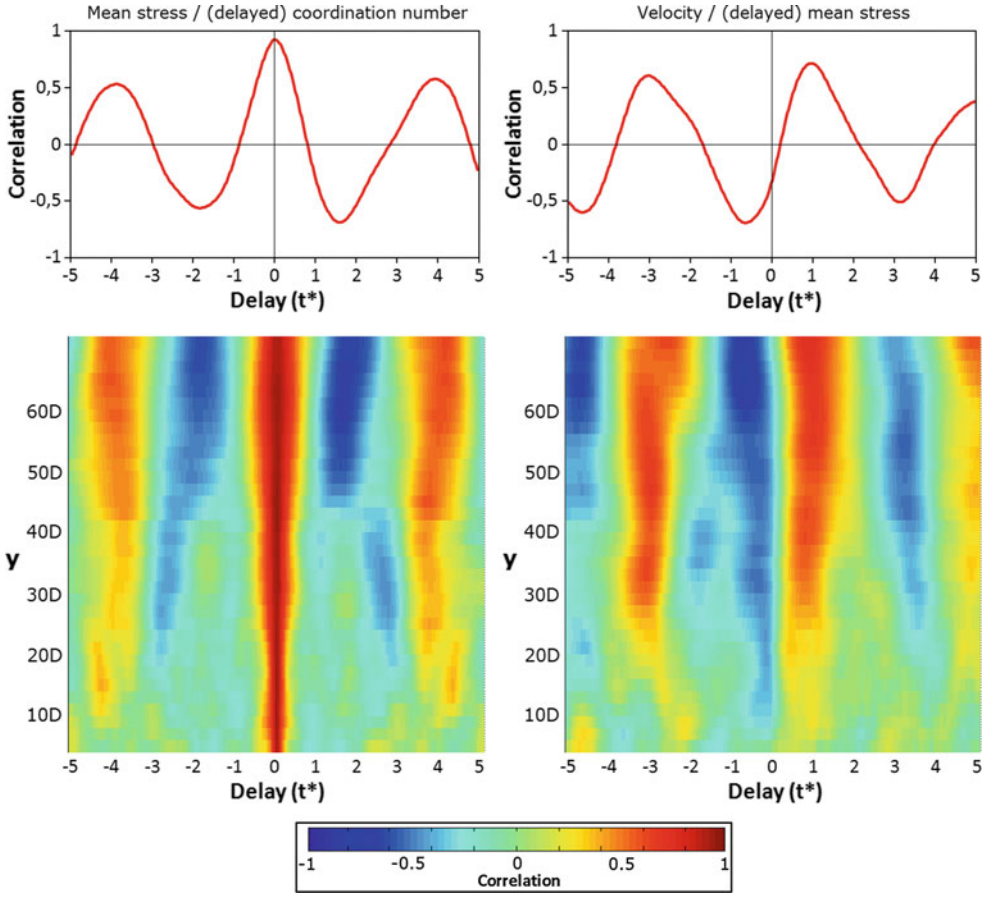

Fig. 8 Delayed correlations. *Left-hand part*: between mean stress and coordination number; *Right-hand part*: between velocity magnitude and mean stress; *Upper part*: for an observation window located at y = 60D; *Lower part*: as a function of the height y of the observation window

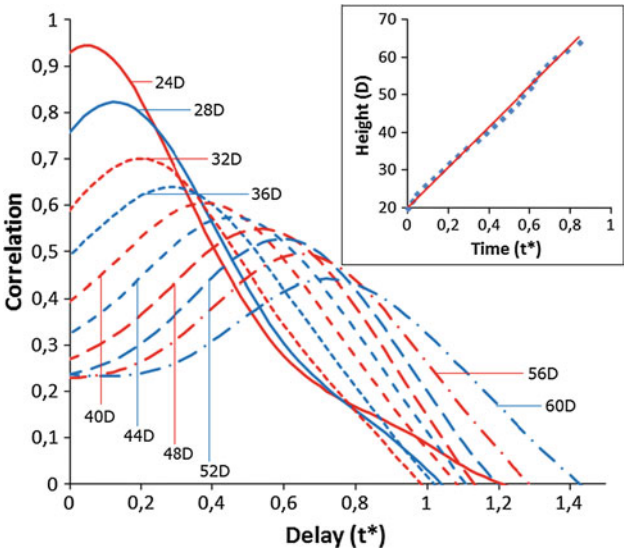

Fig. 9 Delayed correlation of the normalized velocity fluctuations at several heights y as compared with the ones at y = 20D. Inset: correspondence between height and time of maximum correlation, and linear fitting

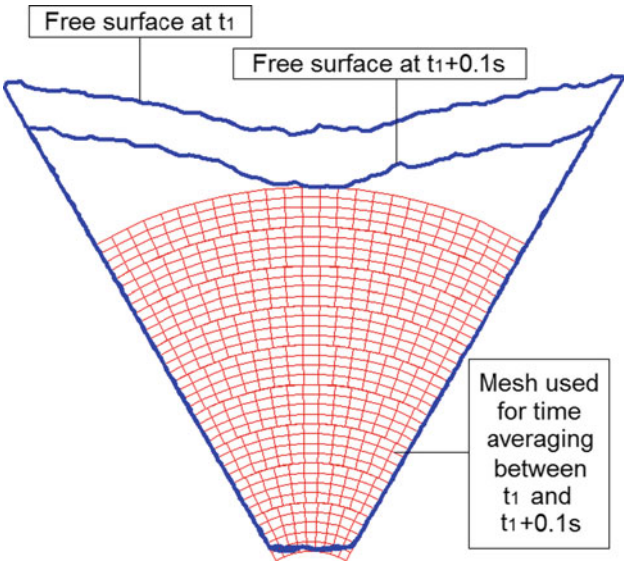

Fig. 10 Radial mesh of the hopper, superimposed to the envelope of the granular mass at the beginning and at the end of the observation time interval

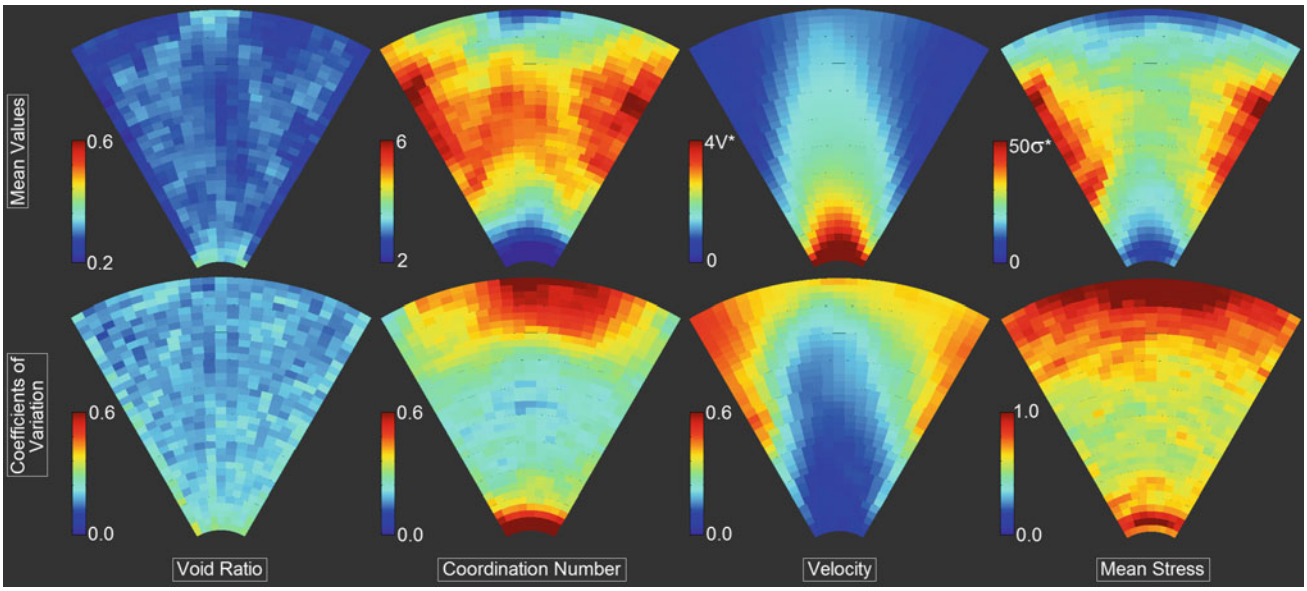

Fig. 11 Fields of the mean values and of the coefficients of variation of t the void ratio, the coordination number, the velocity magnitude, and the mean stress, in the whole hopper

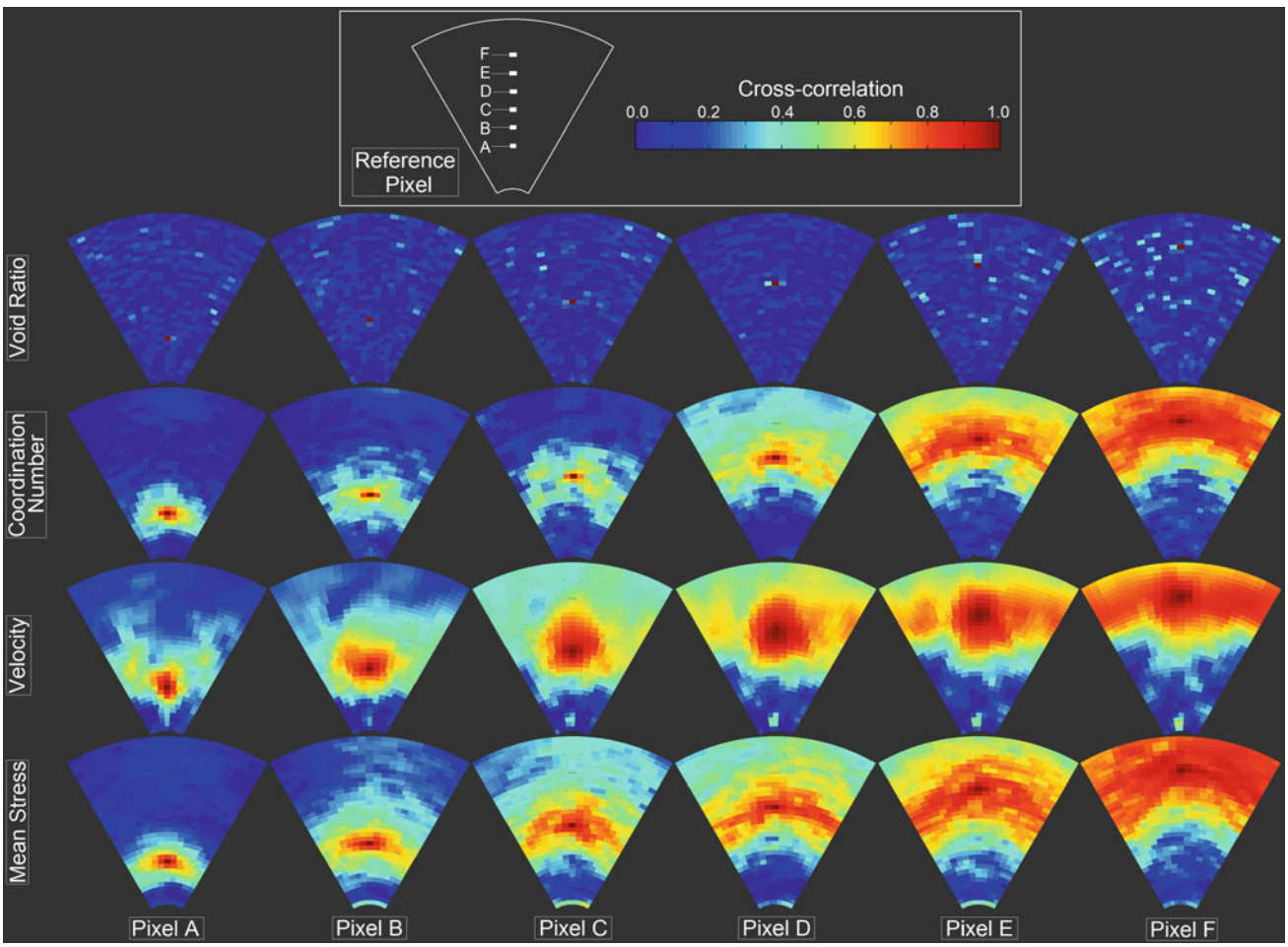

Fig. 12 Spatial cross-correlations of the normalized fluctuations of the void ratio, the coordination number, the velocity magnitude, and the mean stress, using different pixels of reference

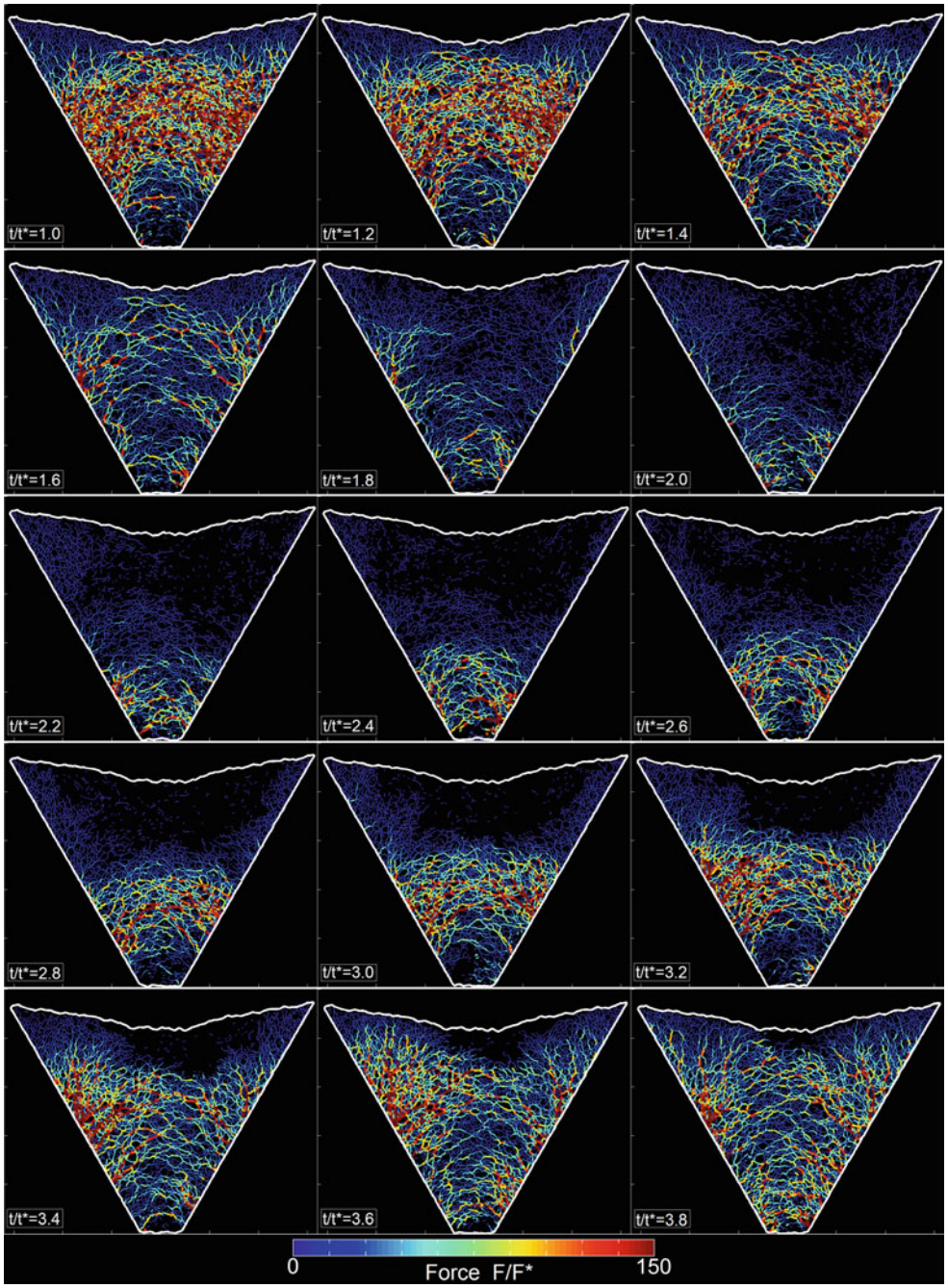

Fig. 13 Evolution of the contact forces network from $t/t^* = 1$ to $t/t^* = 3.8$. The contact forces are represented by segments joining the centres of the particles in contact, the width and color of these segments denoting the load carried by the contact

not carry much load). From $t/t^* = 1.2$ to $t/t^* = 2.0$ the arches appear to gradually dissipate downwards, leaving an almost contact-free state (or free-falling zone) in the entire hopper at $t/t^* = 2.0$ except some persistent long contact force chains near the funnel outlet and along the upper-left part of the hopper. This instant also marks the incipient of a new generation of intense contact force network with similar arching patterns, starting from the lower portion of the hopper close to the outlet to the upper part of the hopper. From $t/t^* = 2.2$ to $t/t^* = 3.2$, these arching pattern network apparently expands in the upward direction, with increasing intensity. During this period, the zone of collisional flow (i.e. flow without persistent contact) in the upper part of the hopper is progressively reduced, while a new contact-free zone seems to develop in the neighborhood of the hopper outlet. The contact force network continues to propagate upwards and becomes more intensified from $t/t^* = 3.4$ to $t/t^* = 3.8$. Meanwhile, new arching network develops close to the outlet.

At $t/t^* = 3.8$, the arching network almost totally occupies the whole hopper. The observations indicate the propagation of a transient stress wave travelling between the hopper outlet and the free surface, and the internal structure of the arching network is rather complex. The properties of this transient stress wave may be an interesting topic for future study.

7 Discussion

Based on a new statistically-based approach on post-processing, the characteristics of fluctuations occurring during the flow of granular particles through a wedge-shaped hopper have been investigated based on DEM simulations using non-spherical particles. The fluctuations in velocity magnitude, mean stress and coordination number all take the form of radial waves propagating upwards from the lower part of the hopper. The waves originate from a height close to $20D$ from the hopper outlet (D being the average grain diameter), and become increasingly harmonic, coordinated and structured when propagating upwards. In the considered case, the wave celerity is close to $50V^*$, and the wave periodicity is close to $4t^*$, leading to a typical wavelength of roughly $200D$. The waves of the mean stress and the coordination number are found perfectly synchronized, and are delayed by roughly t^* with respect to that of velocity magnitude.

The characteristic of local granular density, expressed here by the void ratio, remains somewhat unclear. While the local void ratio is obviously fluctuating during the flow, the fluctuations do not bear an explicit correlation to the main fluctuation patterns of the coordination number, the velocity magnitude or the mean stress. The fluctuation characteristics of void ratio do not show any interesting periodic feature or spatial correlation as observed in the other three quantities. This is somewhat counter-intuitive since one would expect such waves in granular flow to be linked to some local decompressions and recompressions of the granular packing. Indeed, the fluctuations in granular flow have sometimes been described as "density waves", due obviously to their similarities with acoustic waves. There is however no consensus being reached regarding this phenomenon. Some researchers confirmed the observation of such density waves (e.g. [15]) while others observed flow fluctuations to occur at a quasi-constant density (e.g. [18]). In connection with the numerical results in the present study, there are three possible explanations on this apparent paradox: (i) this "acoustic" intuition may be potentially incorrect and there may be no connection between granular density and the observed waves at all, (ii) the system size (only 6,000 particles, and a total vertical size of roughly $80D$) may not be sufficient for the density waves to fully develop and to be identifiable, or (iii) density waves may indeed exist but the chosen post-processing methods cannot detect them. The second explanation may be relatively easy to be verified by conducting larger-scale discrete simulations in the future. Regarding the third possibility, this paper indicates the existence of persistent granular arrangements with rather constant local density moving downwards with the flow (Fig. 5). Thus, even without any flow fluctuations, the void ratio field is never constant in time at a given location in the hopper. These structures may be hiding some possible density waves with small amplitudes propagating upwards, with which a more accurate post-processing technique may be needed to reveal these structures and to identify the possible underlying fluctuation waves.

As mentioned before, though multiple realizations of the hopper flow can help to ensure the statistical consistency of the characteristics of the treated quantities, the major results presented in the current study remain justifiable because of the long duration of the simulated flow. This duration (roughly $120t^*$) is indeed important when compared to the typical period of a fluctuation (roughly $4t^*$), and to the time window considered for the time-correlation analyses (the relevant correlations are between $-t^*$ and t^*). To render the numerical results more relevant, a refilling method for the discharge (i.e., all discharged particles being refilled into the hopper at the moment they exit from the outlet) is suggested to get rid of the transient character of the flow and turn the discharge into a steady flow.

The statistical methodological framework presented in this paper provides a rational and robust way to quantify the spatial and temporal fluctuations of chosen quantities in a hopper granular flow and to identify the most relevant characteristics. It is general too since it may be applied to any other kind of granular flow. Though described in 2D only, this framework may be readily extended to the 3D case since no extra conceptual complications are indeed needed. There are meanwhile additional questions to be addressed. For example, one may question the potential links between the fundamental properties of the observed waves (frequency, celerity, amplitude, synchronization on the way upward, etc.) and the geometry of the hopper (opening angle, opening width, filling height) and/or the characteristics of the granular material (size distribution, complexity of the grains shapes, etc.). A number of parametric studies are indeed meaningful to confirm the general trends observed by some existing studies (e.g. an increase of the wave celerity with decreasing opening angle, or a decrease of the fluctuations amplitude with rounder particles, etc.). Our future work will be dedicated to deal with these questions, and to find some micromechanical explanations for such trends (in detailed consideration of such properties of the force chains and arches as the length, duration, strength, etc.). A generalization of this problem into a fully three-dimensional framework is also desirable. A framework for generating realistic 3D grains was proposed recently by

the present authors (see [31]), but the complete method of generation of a realistic 3D granular sample is still to be defined.

Acknowledgments We appreciate the constructive comments offered by the two anonymous reviewers. The study was supported by Research Grants Council of Hong Kong (under RGC/GRF 622910).

References

1. Forterre, Y., Pouliquen, O.: Flows of dense granular media. Annu. Rev. Fluid Mech. **40**, 1–24 (2008)
2. Cundall, P.A., Strack, O.D.L.: A discrete numerical model for granular Assemblies. Geotechnique **29**, 47–65 (1979)
3. McDowel, G., Li, H., Lowndes, I.: The importance of particle shape in discrete-element modelling of particle flow in a chute. Géotech. Lett. **1**(3), 59–64 (2011)
4. Peng, G., Herrmann, J.: Density waves and 1/f density fluctuations in granular flow. Phys. Rev. E **51**(3), 1745–1756 (1995)
5. Baran, O., Halsey, T., Grest, G.S., Lechman, J.B.: Velocity correlations in dense gravity-driven granular chute flow. Phys. Rev. E **74**, 051302 (2006)
6. Azema, E., Descantes, Y., Roquet, N., Roux, J.-N., Chevoir, F.: Discrete simulation of dense flows of polyhedral grains down a rough inclined plane. Phys. Rev. E **86**, 031303 (2012)
7. Richefeu, V., Mollon, G., Daudon, D., Villard, P.: Dissipative contacts and realistic block shapes for modelling rock avalanches. Eng. Geol. **149–150**, 78–92 (2012)
8. Mollon, G., Richefeu, V., Villard, P., Daudon, D.: Numerical simulation of rock avalanches: influence of a local dissipative contact model on the collective behavior of granular flows. J. Geophys. Res. Solid Earth **117**, F02036 (2012)
9. Zhu, H.P., Yu, A.B.: Steady-state granular flow in a 3D cylindrical hopper with flat bottom: macroscopic analysis. Granul. Matt. **7**, 97–107 (2005)
10. Nguyen, T.V., Brennen, C., Sabersky, R.H.: Gravity flow of granular materials in conical hoppers. J. Appl. Mech. **46**, 529–535 (1979)
11. Bazant, M.Z.: A theory of cooperative diffusion in dense granular flows. arXiv:cond-mat/0307379v2 (2004)
12. Hendy, S.: Instabilities in granular flows. arXiv:cond-mat/0007236v1 (2008)
13. Sun, J., Sundaresan, S.: Radial hopper flow prediction using constitutive model with microstructure, evolution. arXiv:1207.1751v1 (2012)
14. Michalowski, R.L.: Flow of granular material through a plane hopper. Powder Technol. **39**, 29–40 (1983)
15. Baxter, G.W., Behringer, R.P., Fagert, T., Johnson, G.A.: Pattern formation in flowing sand. Phys. Rev. Lett. **62**(24), 2825–2828 (1989)
16. Choi, J., Kudrolli, A., Bazant, M.Z.: Velocity profile of granular flows inside silos and hoppers. J. Phys. Condens. Matt. **17**, S2533–S2548 (2005)
17. Gardel, E., Keene, E., Dragulin, S., Easwar, N., Menon, N.: Force-velocity correlations in a dense, collisional, granular flow. arXiv:cond-mat/0601022 (2006)
18. Gardel, E., Seitaridou, E., Facto, K., Keene, E., Hattam, K., Easwar, N., Menon, N.: Dynamical fluctuations in dense granular flows. Philos. Trans. R. Soc. A **367**, 5109–5121 (2009)
19. Gentzler, M., Tardos, G.I.: Measurement of velocity and density profiles in discharging conical hoppers by NMR imaging. Chem. Eng. Sci. **64**, 4463–4469 (2009)
20. Vivanco, F., Rica, S., Melo, F.: Dynamical arching in a two dimensional granular flow. Granul. Matt. **14**(5), 563–576 (2012)
21. Ristow, G.H., Herrmann, H.J.: Density patterns in two-dimensional hoppers. Phys. Rev. E **50**(1), R5–R8 (1994)
22. Potapov, A., Campbel, C.S.: Computer simulation of hopper flow. Phys. Fluids **8**(11), 2884–2894 (1996)
23. Cleary, P.W., Sawley, M.L.: DEM modelling of industrial granular flows: 3D case studies and the effect of particle shape on hopper discharge. Appl. Math. Model. **26**, 89–111 (2002)
24. Radjai, F., Roux, S.: Turbulentlike fluctuations in quasistatic flow of granular media. Phys. Rev. Lett. **89**(6), 064302 (2002)
25. Richefeu, V., Combe, G., Viggiani, G.: An experimental assessment of displacement fluctuations in a 2D granular material subjected to shear. Géotech. Lett. **2**, 113–118 (2012)
26. Abedi, S., Rechenmacher, A.L., Orlando, A.D.: Vortex formation and dissolution in sheared sands. Granul. Matt. **14**, 695–705 (2012)
27. Mollon, G., Zhao, J.: Fourier-Voronoi-based generation of realistic samples for discrete modelling of granular materials. Granul. Matt. **14**(5), 621–638 (2012)
28. Das, N.: Modeling three-dimensional shape of sand grains using discrete element method. PhD Thesis, University of South Florida, 149 p. (2007)
29. Ferellec, J.-F., McDowell, G.: A method to model realistic particle shape and inertia in DEM. Granul. Matt. **12**, 459–467 (2010)
30. Mollon, G., Zhao, J.: The influence of particle shape on granular hopper flow. In: Powders and Grains 2013: AIP Conference Proceedings 1542, pp. 690–693. doi:10.1063/1.4812025 (2013)
31. Mollon, G., Zhao, J.: Generating realistic 3D sand particles using Fourier descriptors. Granul. Matt. **15**(1), 95–108 (2013)